New Phytologist

Research

Tomato geranylgeranyl diphosphate synthase isoform 1 is involved in the stress-triggered production of diterpenes in leaves and strigolactones in roots

Miguel Ezquerro[1,2], Changsheng Li[3], Julia Pérez-Pérez[1], Esteban Burbano-Erazo[1], M. Victoria Barja[2], Yanting Wang[3], Lemeng Dong[3], Purificación Lisón[1], M. Pilar López-Gresa[1], Harro J. Bouwmeester[3] and Manuel Rodríguez-Concepción[1]

[1]Institute for Plant Molecular and Cell Biology (IBMCP), CSIC-Universitat Politècnica de València, Valencia, 46022, Spain; [2]Centre for Research in Agricultural Genomics (CRAG) CSIC-IRTA-UAB-UB, Campus UAB Bellaterra, Barcelona, 08193, Spain; [3]Plant Hormone Biology Group, Green Life Sciences Cluster, Swammerdam Institute for Life Sciences, University of Amsterdam, Science Park 904, Amsterdam, 1098 XH, the Netherlands

Author for correspondence:
Manuel Rodríguez-Concepción
Email: manuelrc@ibmcp.upv.es

Received: *9 May 2023*
Accepted: *5 June 2023*

New Phytologist (2023)
doi: 10.1111/nph.19109

Key words: abscisic acid (ABA), carotenoid, diterpenes, geranylgeranyl diphosphate (GGPP), phytoene synthase, strigolactones.

Summary

- Carotenoids are photoprotectant pigments and precursors of hormones such as strigolactones (SL). Carotenoids are produced in plastids from geranylgeranyl diphosphate (GGPP), which is diverted to the carotenoid pathway by phytoene synthase (PSY). In tomato (*Solanum lycopersicum*), three genes encode plastid-targeted GGPP synthases (*SlG1* to *SlG3*) and three genes encode PSY isoforms (*PSY1* to *PSY3*).
- Here, we investigated the function of SlG1 by generating loss-of-function lines and combining their metabolic and physiological phenotyping with gene co-expression and co-immunoprecipitation analyses.
- Leaves and fruits of *slg1* lines showed a wild-type phenotype in terms of carotenoid accumulation, photosynthesis, and development under normal growth conditions. In response to bacterial infection, however, *slg1* leaves produced lower levels of defensive GGPP-derived diterpenoids. In roots, *SlG1* was co-expressed with *PSY3* and other genes involved in SL production, and *slg1* lines grown under phosphate starvation exuded less SLs. However, *slg1* plants did not display the branched shoot phenotype observed in other SL-defective mutants. At the protein level, SlG1 physically interacted with the root-specific PSY3 isoform but not with PSY1 and PSY2.
- Our results confirm specific roles for SlG1 in producing GGPP for defensive diterpenoids in leaves and carotenoid-derived SLs (in combination with PSY3) in roots.

Introduction

Isoprenoids are one of the most diverse families of compounds in all living organisms, with plants displaying the highest functional and structural variation (Bouvier *et al.*, 2005). The universal building blocks for the biosynthesis of all isoprenoids are isopentenyl diphosphate (IPP) and its allylic isomer dimethylallyl diphosphate (DMAPP). Both five-carbon (C_5) isoprenoid-building molecules are produced in plants by the mevalonic acid (MVA) pathway in the cytosol and the methylerythritol 4-phosphate (MEP) pathway in plastids (Pulido *et al.*, 2012; Tholl, 2015). Condensation of one or more molecules of IPP to one molecule of DMAPP produces C_{10} geranyl diphosphate (GPP), C_{15} farnesyl diphosphate (FPP), and C_{20} geranylgeranyl diphosphate (GGPP), which are the precursors for most downstream isoprenoid compounds in different cell compartments (Ruiz-Sola & Rodríguez-Concepción, 2012; Zhou & Pichersky, 2020). In the cytosol, FPP is used to synthesize C_{15} sesquiterpenes and C_{30} triterpenes required for normal plant growth, defensive responses, membrane structure, and prenylation of proteins (Thulasiram & Poulter, 2006). In the plastids, GPP is used to make C_{10} monoterpenes (mostly volatile compounds related to aroma and plant–pathogen interactions) (Degenhardt *et al.*, 2009; Chen *et al.*, 2015) and GGPP is the precursor of C_{20} diterpenes, gibberellins (GAs) and several photosynthesis-related isoprenoids such as carotenoids, tocopherols, chlorophylls, plastoquinone, and phylloquinones (Barja & Rodriguez-Concepcion, 2021). GGPP is also used to produce diterpenes in the cytosol, and both FPP and GGPP are produced in mitochondria from imported MVA-derived IPP and DMAPP for ubiquinone and diterpene biosynthesis (Thulasiram & Poulter, 2006; Barja & Rodriguez-Concepcion, 2021).

C_{40} carotenoids are GGPP-derived plastidial isoprenoids that function as precursors of vitamin A and health-promoting

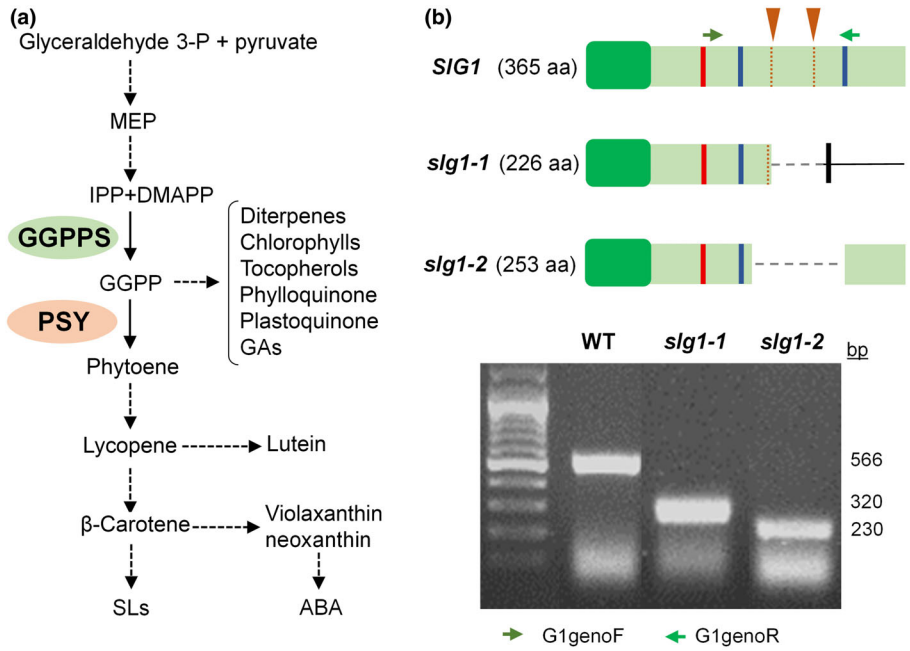

Fig. 1 Carotenoid pathway and tomato mutants. (a) Carotenoid biosynthesis pathway. Dashed arrows represent multiple steps. The reactions catalyzed by geranylgeranyl diphosphate synthase (GGPPS) and phytoene synthase (PSY) are marked. (b) Scheme representing the wild-type SlG1 protein and the mutant versions generated in the corresponding CRISPR-Cas9-generated alleles (see Supporting Information Figs S1, S2 for further details). Dark green boxes represent plastid transit peptides. The regions targeted by the designed sgRNAs are indicated with orange arrowheads and dotted lines. Red and blue bars mark the position of conserved domains required for GGPPS activity (protein–protein interaction domains and Asp-rich domains, respectively). Deletions are shown with a dashed line. Green arrows represent the position of primers for PCR-based genotyping. The agarose gel shows the PCR genotyping products using these primers. ABA, abscisic acid; DMAPP, dimethylallyl diphosphate; GA, gibberellins; IPP, isopentenyl diphosphate; MEP, methylerythritol 4-phosphate; SL, strigolactones; WT, wild-type.

phytonutrients in the human diet and have a great industrial interest as natural pigments (Ruiz-Sola & Rodríguez-Concepción, 2012; Rodriguez-Concepcion *et al.*, 2018). In plants, carotenoids act as photoprotectors in leaves, as pigments in the flowers and fruits of many plant species and as precursors of apocarotenoids, including bioactive compounds such as the hormones abscisic acid (ABA) and strigolactones (SLs) (Al-Babili & Bouwmeester, 2015; Rodriguez-Concepcion *et al.*, 2018). Despite their biological and economic relevance, the factors that integrate and coordinate carotenoid biosynthesis with plant metabolism and development remain little known. In this context, understanding how GGPP is channeled to the production of carotenoids for particular functions in diverse tissues, developmental stages, and environmental conditions remains a pivotal question.

In plastids, GGPP is produced from MEP-derived IPP and DMAPP by GGPP synthase (GGPPS) enzymes. The first committed and main flux-controlling step of the carotenoid biosynthesis pathway is the condensation of two molecules of GGPP into phytoene catalyzed by phytoene synthase (PSY). Next, phytoene is desaturated and isomerized to lycopene, and the ends of the linear lycopene chain are cyclized to form β-carotene (with two β rings) or α-carotene (with one β and one ε ring). Oxidation of the rings gives rise to xanthophylls such as violaxanthin and neoxanthin from β-carotene or lutein from α-carotene (Fig. 1a; Rodriguez-Concepcion *et al.*, 2018).

In the model plant *Arabidopsis thaliana*, PSY is encoded by one gene and the resulting protein directly interacts with AtG11, the main plastidial GGPPS. This interaction likely facilitates the channeling of GGPP to the production of carotenoids (Ruiz-Sola *et al.*, 2016a,b; Camagna *et al.*, 2019). A more complex scenario is found in tomato (*Solanum lycopersicum*). The extra roles associated with carotenoids in this species compared with Arabidopsis (including flower and fruit pigmentation and root mycorrhiza formation) together with genome duplication events have resulted in small PSY and GGPPS gene families. With regard to PSY, tomato has an isoform with a primary role in pigmentation of flowers and ripe fruit (PSY1, Solyc03g031860), another one mainly involved in the production of carotenoids for photosynthesis and photoprotection in leaves (PSY2, Solyc02g081330) and a third one associated with SL and apocarotenoid biosynthesis in roots (PSY3, Solyc01g005940) (Stauder *et al.*, 2018; Ezquerro *et al.*, 2022). From the three plastid-targeted GGPPS isoforms identified in tomato, herein referred to as SlG1 (Solyc11g011240), SlG2 (Solyc04g079960), and SlG3 (Solyc02g085700) (Zhou & Pichersky, 2020; Barja *et al.*, 2021), only SlG2 and SlG3 have been studied in detail. They both produce GGPP for carotenoid synthesis in leaves and fruits, with SlG3 being the main housekeeping isoform and SlG2 acting as a helper enzyme to meet peak demands of GGPP in both organs. SlG2 can be co-immunoprecipitated with both PSY1 and PSY2, but SlG3 cannot (Barja *et al.*, 2021). Although SlG1 is also an active plastid-targeted GGPPS enzyme (Zhou & Pichersky, 2020; Barja *et al.*, 2021), it cannot complement the loss of SlG2 and SlG3 in double mutants, which show an embryo-lethal

phenotype like that reported for AtG11-defective Arabidopsis mutants (Ruiz-Sola *et al.*, 2016a,b; Barja *et al.*, 2021). Indeed, *SlG1* transcripts are much less abundant than those of *SlG2* and *SlG3* in most plant tissues (Zhou & Pichersky, 2020; Barja *et al.*, 2021). In leaves, *SlG1* expression is normally low but it is induced following spider mite feeding, wounding, and elicitor treatments correlating with the production of defense-related diterpenoid volatiles (Ament *et al.*, 2006). Other gene expression data suggest that SlG1 might have a role in roots during mycorrhiza formation (Stauder *et al.*, 2018; Barja *et al.*, 2021).

Under nitrogen and/or phosphate starvation, the roots of many plant species (including tomato) exude large quantities of carotenoid-derived SLs to promote recognition and colonization by arbuscular mycorrhizal (AM) fungi (Yoneyama *et al.*, 2008; Zhang *et al.*, 2014; Matthys *et al.*, 2016; Stauder *et al.*, 2018). These symbiotic AM fungi help the plant by facilitating access to water and mineral nutrients in poor soils, in exchange for carbon products biosynthesized by the plant (Bouwmeester *et al.*, 2007; Yoneyama *et al.*, 2008). Carotenoid metabolism is in turn stimulated in AM roots, resulting in the production of high amounts of pigments such as mycorrhadicins and other apocarotenoids including blumenols, zaxinone, and anchorene that modulate the establishment of the AM symbiosis and rhizospheric interactions (Fester *et al.*, 2002; Baslam *et al.*, 2013; Stauder *et al.*, 2018; Moreno *et al.*, 2021). *SlG1* and *PSY3* have been proposed to play a coordinated role for SL and AM-associated apocarotenoid biosynthesis in roots, mainly based on expression data (Stauder *et al.*, 2018; Barja *et al.*, 2021). *SlG1* and *PSY3* are indeed the most highly upregulated genes encoding GGPPS and PSY isoforms when roots are mycorrhized. However, *SlG2* and *PSY1* also show increased transcript levels in mycorrhized roots compared with nonmycorrhized controls (Stauder *et al.*, 2018; Barja *et al.*, 2021). This, together with the observation that the basal expression levels of *SlG1* and *PSY3* in roots are lower than those of *SlG2* and *PSY1* (Fantini *et al.*, 2013; Barja *et al.*, 2021), suggests that more than one isoform of these two enzymes might be providing precursors for carotenoids and derived compounds in roots. To experimentally test this hypothesis and better understand the biological role of SlG1 in tomato, we created CRISPR-Cas9-edited lines defective in SlG1. Here, we report their generation and characterization. We provide experimental evidence demonstrating a role for tomato SlG1 in the production of defense-associated diterpenes in leaves and the existence of a highly specific SlG1-PSY3 module to produce SLs in the roots.

Materials and Methods

Plant material

Tomato (*S. lycopersicum* L. var. MicroTom) plants were used for experiments. The *ccd7* line, previously referred to as *CCD7-AS*, was made by introgressing a construct expressing a *CCD7* antisense from M82 (Vogel *et al.*, 2010) into MicroTom by successive backcrosses (Pino *et al.*, 2022). Seeds were surface-sterilized by a 30-min water wash followed by a 15-min incubation in 10 ml of 40% bleach with 10 µl of Tween-20. After three consecutive 10 min washes with sterile milli-Q water, seeds were germinated on plates with solid 0.5× Murashige & Skoog (MS) medium containing 1% agar (without vitamins or sucrose). The medium was supplemented with kanamycin (100 µg ml^{-1}) when required to select transgenic plants. Plates were incubated in a climate-controlled growth chamber (Ibercex, Madrid, Spain) at 26°C with a photoperiod of 14 h of white light (photon flux density of 50 µmol m^{-2} s^{-1}) and 10 h of darkness. After 10–14 d, seedlings were transferred to soil and grown under standard glasshouse conditions (14 h : 10 h, 25 ± 1°C : 22 ± 1°C, light : dark). Plants used for root metabolic analysis were grown in a glasshouse with the same conditions but in a mixture of river sand (0.5–1 mm; Filcom BV, Papendrecht, the Netherlands) and a clay granulate (1 : 1) instead of soil for easier root collection. For the analysis of phenotypical traits influenced by SLs, 15 plants were grown for 4 wk under half-strength Hoagland solution and then for 2 additional weeks under half-strength Hoagland solution without PO_4^{-3}. For experiments testing root phenotypes in seedlings, seeds were germinated on MS medium lacking KH_2PO_4 in large square (245 mm) Petri dishes that were incubated vertically for 2 wk in the growth chamber. The lower section of the dishes was covered with aluminum foil, so only the shoots were directly exposed to light. *Nicotiana benthamiana* Domin plants used for co-immunoprecipitation experiments were grown in the glasshouse under long-day conditions at 24°C for 21 d.

Sample collection and phenotypical analyses

Young leaf samples correspond to growing leaflets from the fifth and sixth true leaves, and they were collected from soil-grown 4-wk-old plants. Chlorophyll fluorescence measurements were carried out with a Handy FluorCam (Photon Systems Instruments, Drásov, Czech Republic). ϕPSII (effective quantum yield of photosystem II) was measured at 30 PAR with an actinic light of 3 µmol m^{-2} s^{-1}. Tomato fruit pericarp samples for isoprenoid quantification were collected 3 d after the breaker (B) stage (B + 3). Roots, leaflets, and pericarp samples were frozen in liquid nitrogen immediately after collection, freeze-dried, and stored at −80°C. For counting the days from breaker to orange stage, 30 fruits ($n = 30$) from each genotype were chosen and their ripening was monitored *in planta*. For fruit weight determination, 100 ripe fruits from each genotype were collected and weighted one by one using a precision scale (Kern, Balingen, Germany). Fruit volume was estimated in 10 pools of 10 fruits each by measuring the displaced water volume in a graduated cylinder. Root phenotypes of seedlings were analyzed using WinRhizo (Régent Instrument Inc., Quebec, QC, Canada) and ImageJ (https://imagej.nih.gov/).

Constructs and tomato transformation

For co-immunoprecipitation experiments, full-length cDNAs encoding SlG1 and PSY3 proteins without their stop codons were amplified from root cDNA using the Phusion High-fidelity DNA polymerase (Thermo Fisher, Waltham, MA, USA). Next, the amplicons were introduced via BP clonase into pDONR207 entry plasmid using Gateway (GW) technology (Invitrogen).

Full-length sequences were then subcloned through an LR reaction into pGWB414 and pGWB420 plasmids as reported previously (Barja *et al.*, 2021). For CRISPR-Cas9-mediated disruption of *SlG1*, two single-guide RNAs (sgRNA; Supporting Information Figs S1, S2) were designed using the online tool CRISPR-P v.2.0 (Liu *et al.*, 2017). Cloning of the CRISPR-Cas9 constructs was carried out as described previously (Barja *et al.*, 2021) using primers listed in Table S1. As a result, a single final binary plasmid harboring the Cas9 sequence, the NPTII gene providing kanamycin resistance, and the sgRNAs were obtained and named pDE-Cas9-SlG1 (Table S2). All constructs were confirmed by restriction mapping and DNA sequencing. *Agrobacterium tumefaciens* GV3101 strain was used to stably transform tomato MicroTom cotyledons with pDE-Cas9-SlG1 as described (Ezquerro *et al.*, 2022). *In vitro* regenerated T1 lines were identified based on kanamycin resistance (100 μg ml^{-1}), PCR genotyping, and sequencing (Table S1). Homozygous T2 lines lacking Cas9 were obtained after segregation, and stable T3 offspring were used for the next experiments.

Metabolite and gene expression analyses

Plastidial isoprenoids (carotenoids, chlorophylls, and tocopherols) were detected by high-performance liquid chromatography coupled to diode array and fluorescence detectors, hormones (ABA, SL) were quantified by liquid chromatography coupled to mass spectrometry (LC–MS), and volatile organic compounds were quantified by gas chromatography coupled to mass spectrometry (GC–MS), as described (Methods S1). Gene co-expression networks were constructed using publicly available data from tomato roots grown in +P and −P conditions (Wang *et al.*, 2021) and tomato homologues for isoprenoid biosynthetic genes as preys (Methods S2). RT-qPCR analyses were performed using gene-specific primers (Table S1) and *ACT4* (Solyc04g011500) as endogenous reference gene as described (Methods S2).

Bacterial infection of tomato plants

Pseudomonas syringae pv *tomato* DC3000 (*Pst*) strain were used for tomato infection as reported previously (López-Gresa *et al.*, 2018). Briefly, bacteria were grown for 48 h at 28°C in LB agar medium with rifampicin (10 μg ml^{-1}) and kanamicin (0.5 μg ml^{-1}). When colonies appeared, they were transferred to King's B liquid medium supplemented with antibiotics and grown overnight at 28°C. Next, bacteria were centrifugated at 3000 ***g*** for 15 min and resuspended in 10 mM $MgCl_2$ at a final optical density of 0.1 for further infection. Inoculation with bacteria was carried out in 4-wk-old MicroTom plants without flowers by immersion. Plants were dipped into the bacterial suspension containing 0.05% Silwet L-77 for 30 s and left for 24 h for subsequent sample collection.

Co-immunoprecipitation assays

Co-immunoprecipitation experiments were carried out using constructs encoding GGPPS and PSY proteins fused to Myc and hemagglutinin (HA) epitopes that were expressed in *N. benthamiana* leaf cells as described (Methods S3).

Results

Generation of CRISPR lines defective in SlG1

The approach followed to create *SlG1*-defective mutants by CRISPR-Cas9 was very similar to the one followed to generate *slg2* and *slg3* mutants (Barja *et al.*, 2021). Briefly, we designed two single-guide RNAs (sgRNA) with CRISPR-P 2.0 (Liu *et al.*, 2017) to create a small deletion that would disrupt the intronless *SlG1* gene (Fig. 1; see Tables S1, S2 for primer and construct details). After transformation of tomato MicroTom plants and genotyping, two independent mutant alleles without Cas9 were selected and named *slg1-1* and *slg1-2* (Fig. 1b). The *slg1-1* allele has a deletion that causes a frameshift and a premature translation stop codon (Figs 1b, S1, S2). The resulting protein lacks the C-terminal region containing the second Asp-rich motif (SARM, essential for prenyl-transferase function), and it is smaller than the wild-type (WT) enzyme (226 aa instead of 365 aa). A longer deletion in the *slg1-2* allele maintains the open reading frame and produces a 253 aa chimeric protein that lacks a fragment of the WT enzyme containing the SARM (Figs 1b, S1, S2). Similar mutations lacking the C-terminal part of the protein and the SARM were previously shown to result in complete loss of GGPPS activity in *slg2* mutants (Barja *et al.*, 2021). Therefore, we considered these two alleles as knockout mutants and selected them for the rest of experiments.

Loss of SlG1 does not impair the production of photosynthesis-related isoprenoids in tomato leaves

SlG1 is expressed at low levels in all tomato plant tissues, including leaves (Fig. S3). To investigate possible roles of SlG1 in leaves, we first analyzed the levels of GGPP-derived plastidial isoprenoids in *slg1* lines under normal growth conditions (Fig. 2). Lines lacking SlG2 (*slg2-1*) or SlG3 (*slg3-1*) were grown together with the SlG1-defective mutants and WT controls for comparison. Young and mature leaves of *slg1-1* and *slg1-2* plants appeared very similar to those from *slg2* and WT plants (Fig. 2a). By contrast, young emerging leaves from *slg3* plants showed a paler green color as reported previously (Barja *et al.*, 2021). The color phenotype of young leaves correlated with their photosynthetic pigment (carotenoids and chlorophylls) content (Fig. 2b), and their photosynthetic activity estimated as effective quantum yield of photosystem II (ϕPSII; Fig. 2c), which were only reduced in the *slg3* mutant. Tocopherol levels, by contrast, were similar in all the lines, although a trend toward lower levels was detected in young leaves of the *slg3* mutant, as reported previously (Barja *et al.*, 2021). The described results are in agreement with our previous conclusion that *SlG3* is the main isoform in supplying GGPP for photosynthesis-related isoprenoids in leaves under normal growth conditions (Barja *et al.*, 2021). A role for SlG2 in providing extra GGPP to support the production of these isoprenoids when needed, for example, during de-etiolation, was

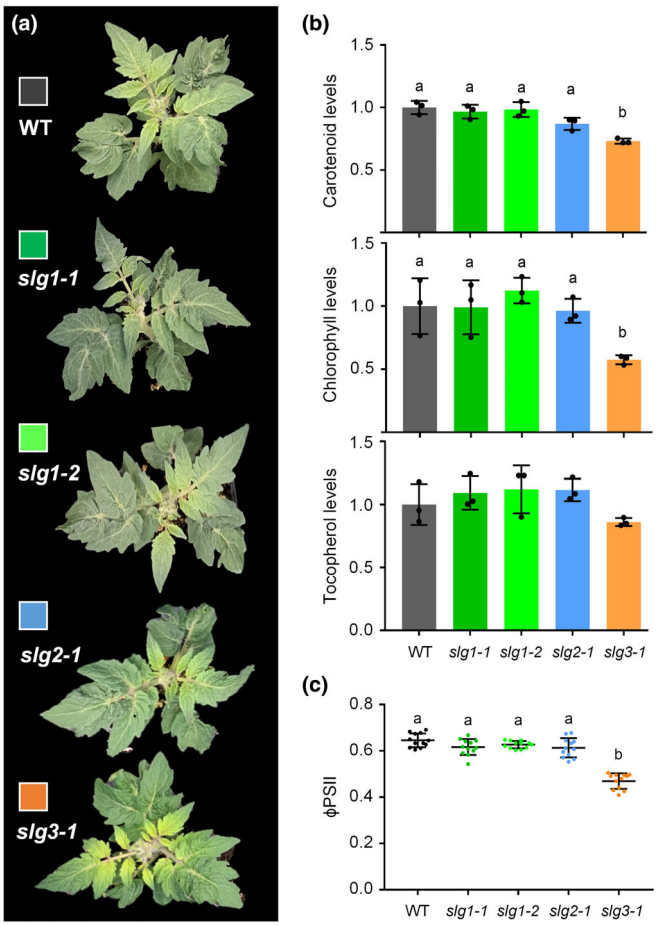

Fig. 2 SlG1 does not contribute to photosynthesis-related isoprenoid biosynthesis in tomato leaves. (a) Representative images of 4-wk-old plants of wild-type (WT) and geranylgeranyl diphosphate synthase (GGPPS)-defective mutants. (b) Carotenoid, chlorophyll, and tocopherol levels in young leaves from 4-wk-old WT and mutant plants. Values are represented relative to WT levels, and they correspond to mean and SD of $n \geq 3$ independent biological replicates. (c) Effective quantum yield of photosystem II (ϕPSII) in young leaves like those used in (b). Individual values (colored dots) as well as mean and SD are shown, and they correspond to four different areas from leaves of three different plants. In all plots, letters represent statistically significant differences ($P < 0.05$) among means according to *post hoc* Tukey's tests run when one-way ANOVA detected different means.

proposed in part based on gene expression data (Barja *et al.*, 2021). Unlike *SlG2*, however, *SlG1* is poorly co-expressed with isoprenoid biosynthetic genes in leaves and it is not induced during seedling de-etiolation (Barja *et al.*, 2021), supporting the conclusion that SlG1 does not substantially contribute to GGPP production in chloroplasts.

SlG1 is involved in stress-induced diterpene biosynthesis in leaves

Leaves are mainly photosynthetic organs, but they also contain cell types lacking chloroplasts. In particular, tomato leaves contain many glandular trichomes formed by nonphotosynthetic cells that produce large amounts of volatile organic compounds (VOCs), including many of isoprenoid origin (Schuurink & Tissier, 2020). *SlG1* but also *SlG2* and *SlG3* are expressed in leaf trichomes (Zhou & Pichersky, 2020). The main isoprenoid VOCs in these trichomes are MVA-derived sesquiterpenes (made from C_{15} FPP) and MEP-derived monoterpenes (made from C_{10} GPP or nerolidol diphosphate, NPP) and diterpenes (made from C_{20} GGPP). A role for SlG1 in the production of GGPP-derived diterpenes was proposed following the observation that *SlG1* expression was induced in tomato leaves by treatments that stimulated the production of the diterpene geranyllinalool (GL) and its volatile C_{16}-homoterpene derivative (*E*,*E*)-4,8,12-trimethyltrideca-1,3,7,11-tetraene (TMTT; Ament *et al.*, 2006). GL is an acyclic diterpene alcohol with a wide distribution in the plant kingdom, often coexisting with TMTT. While the role of GL itself is not well known, TMTT is a component of volatile blends constitutively released from flowers and emitted by vegetative tissues upon biotic challenge – including mechanical wounding and herbivore feeding – or elicitation with defense-related hormones (Ament *et al.*, 2006; Falara *et al.*, 2014). Besides contributing to the attraction of pollinators, TMTT has been shown to have a defensive role, often as a stress-responsive signal that enables plant-to-plant communication. Our data mining of the database Genevestigator found that *SlG1* expression is also upregulated in leaves after infection with the bacterium *P. syringae* pv *tomato* DC3000 (*Pst*), whereas *SlG2* and *SlG3* transcript levels remained unchanged (Fig. S4). Interestingly, the gene encoding GL synthase (GLS, Solyc03g006550), the enzyme that converts GGPP into GL (Falara *et al.*, 2014), is also upregulated under these conditions (Fig. S4). To investigate whether biotic stress resulting from bacterial infection can also trigger the production of GL and TMTT and explore the role of SlG1 and other GGPPS isoforms in the process, we quantified the expression of genes encoding GLS and GGPPS isoforms (Fig. 3a) and the levels of GL and TMTT (Fig. 3b) in WT and mutant plants 24 h after infection with *Pst* or inoculation with a mock solution. *SlG1* and *GLS* transcript levels were higher in infected leaves, whereas those of *SlG2* and *SlG3* were similar in mock and *Pst*-infected samples (Fig. 3a), in agreement with Genevestigator data (Fig. S4). In all the lines tested, GL and TMTT were virtually undetectable in mock samples but accumulated in infected leaves (Fig. 3b). While *slg2* produced GL and TMTT to levels similar to those of WT controls, they were strongly reduced in *slg1* and *slg3* leaves (Fig. 3c). These results suggest that upregulation of SlG1 helps the housekeeping isoform SlG3 to meet the peak demand of GGPP for diterpene biosynthesis in response to biotic stress, providing genetic evidence for the biological role of SlG1 in leaf diterpene production.

SlG1 is dispensable for carotenoid biosynthesis in fruit

Carotenoids are synthesized at very high rates during tomato fruit ripening, contributing together with the degradation of chlorophylls to progressively change the fruit color from green at the mature green (MG) stage to orange (O) and eventually red at the ripe (R) stage. The first visual symptoms of color change define the breaker (B) stage. *SlG1* is expressed at very low levels during

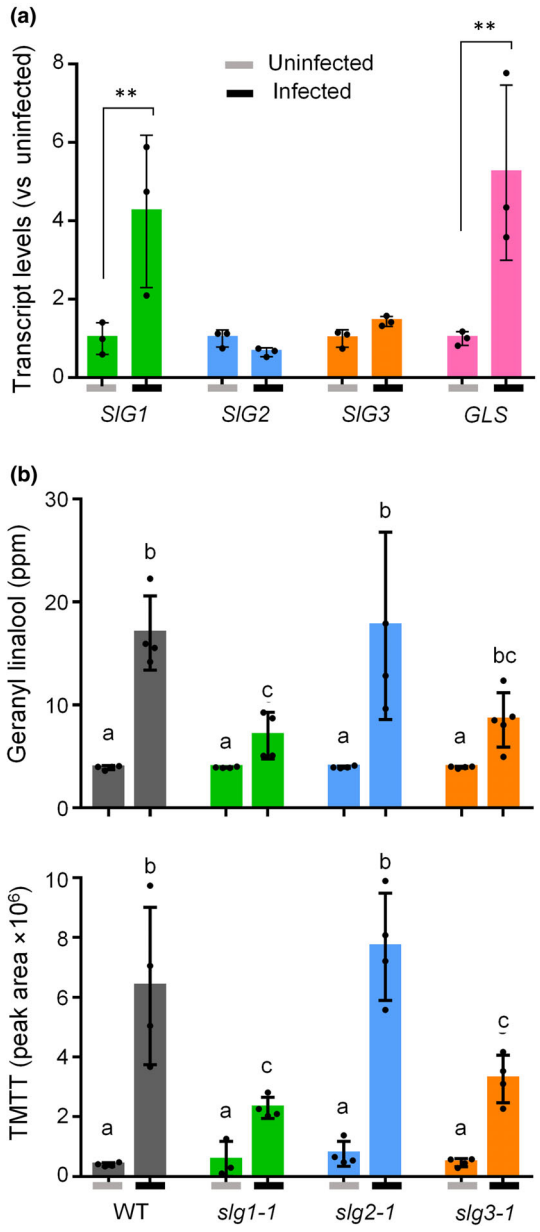

Fig. 3 SlG1 contributes to diterpene production in stressed tomato leaves. MicroTom wild-type (WT) and edited plants were infected with *Pseudomonas syringae* pv *tomato* DC3000 or inoculated with a mock solution and samples were collected 24 h later. (a) RT-qPCR expression data of the indicated genes in WT leaves. Expression levels are shown relative to mock (uninfected) samples, and they correspond to the mean ± SD of $n = 3$ independent biological replicates. Asterisks (**) indicate statistically significant differences among means between uninfected and infected samples (*t*-test: $P < 0.01$). (b) Levels of representative diterpenes in infected and uninfected leaves of WT and geranylgeranyl diphosphate synthase (GGPPS)-defective mutants. Data are represented relative to the levels in uninfected WT samples (100%) and correspond to the mean ± SD of $n = 4$ biological replicates. Letters represent statistically significant differences (one-way ANOVA followed by Tukey's multiple comparisons test: $P < 0.05$). In all the plots, black dots mark individual data values. TMTT, (E, E)-4,8,12-trimethyltrideca-1,3,7,11-tetraene.

fruit ripening (Fig. S3), when GGPP produced by SlG3 and upregulated levels of *SlG2* support carotenoid overproduction (Barja *et al.*, 2021). Reduced activity of SlG2 or SlG3 results in lower levels of lycopene (the main carotenoid accumulated during ripening) in R fruit collected at 10 d after the B stage (B + 10), but only SlG3-defective lines showed significantly decreased levels of total carotenoids at this stage, and none of the mutants showed differences with the WT in MG fruit (Barja *et al.*, 2021). When we measured carotenoid levels in B + 3 fruits (i.e. between O and R stages), WT levels of total carotenoids were found in *slg1* and *slg2* lines, whereas *slg3* fruits showed significantly lower levels (Fig. 4a). In particular, phytoene and lycopene contents were strongly reduced in *slg3* fruits, whereas β-carotene levels were similar to those of WT controls (Fig. 4a). These results suggest that reduced GGPP supply due to loss of SlG3 activity has a stronger impact on the production of the earlier intermediates of the carotenoid pathway that is somehow compensated in downstream steps. The absence of significant differences in carotenoid levels among WT, *slg1*, and *slg2* fruits (Fig. 4a) suggests that SlG3 is the main GGPP provider in the early stages of fruit ripening. As ripening advances, upregulation of SlG2 contributes with extra GGPP. The WT phenotype of SlG1-deficient mutant fruits together with the lack of gene expression changes during ripening support the conclusion that this isoform does not contribute to GGPP for carotenoid production in fruit.

Lower levels of the carotenoid-derived hormone ABA were measured in the fruit pericarp of tomato mutants lacking SlG2 and particularly SlG3, eventually contributing to a delay in ripening (Barja *et al.*, 2021). Consistently, the number of days that B fruits needed to reach the O stage was higher in *slg2* and *slg3* lines compared with WT controls (Fig. 4b). ABA has also been shown to promote fruit growth (Zhang *et al.*, 2009; McQuinn *et al.*, 2020; Ezquerro *et al.*, 2022). Reduced ABA contents in *slg2* and *slg3* fruit pericarp (Barja *et al.*, 2021) actually correlate with a reduced fruit volume of ripe fruit, although this was only statistically significant for *slg3* fruits and it did not affect fruit weight (Fig. 4c). Again, *slg1* fruits were undistinguishable from WT controls (Fig. 4c). The observation that losing SlG1 activity does not impact any of the fruit phenotypes tested strongly supports the conclusion that this isoform is dispensable for the production of GGPP for carotenoids and related metabolites during fruit ripening.

Gene co-expression analysis suggests a major role for SlG1 in roots

In our previous work, we demonstrated that *SlG2* and, to a lower extent, *SlG3* expression were highly correlated to the expression of plastidial isoprenoid biosynthetic genes in leaf tissue. In fruits, *SlG3* expression is more correlated than that of *SlG2* to genes from these metabolic pathways (Barja *et al.*, 2021). The correlation of *SlG1* with other plastidial isoprenoid genes was very poor in leaves and in fruits. Other gene expression data suggested that *SlG1* might function in roots to produce SL or/and AM-related apocarotenoids (Stauder *et al.*, 2018; Barja *et al.*, 2021). To provide further evidence for this hypothesis, we performed a gene co-expression network (GCN) analysis in roots. We used publicly available data for plant comparative genomics (PLAZA v.4.0

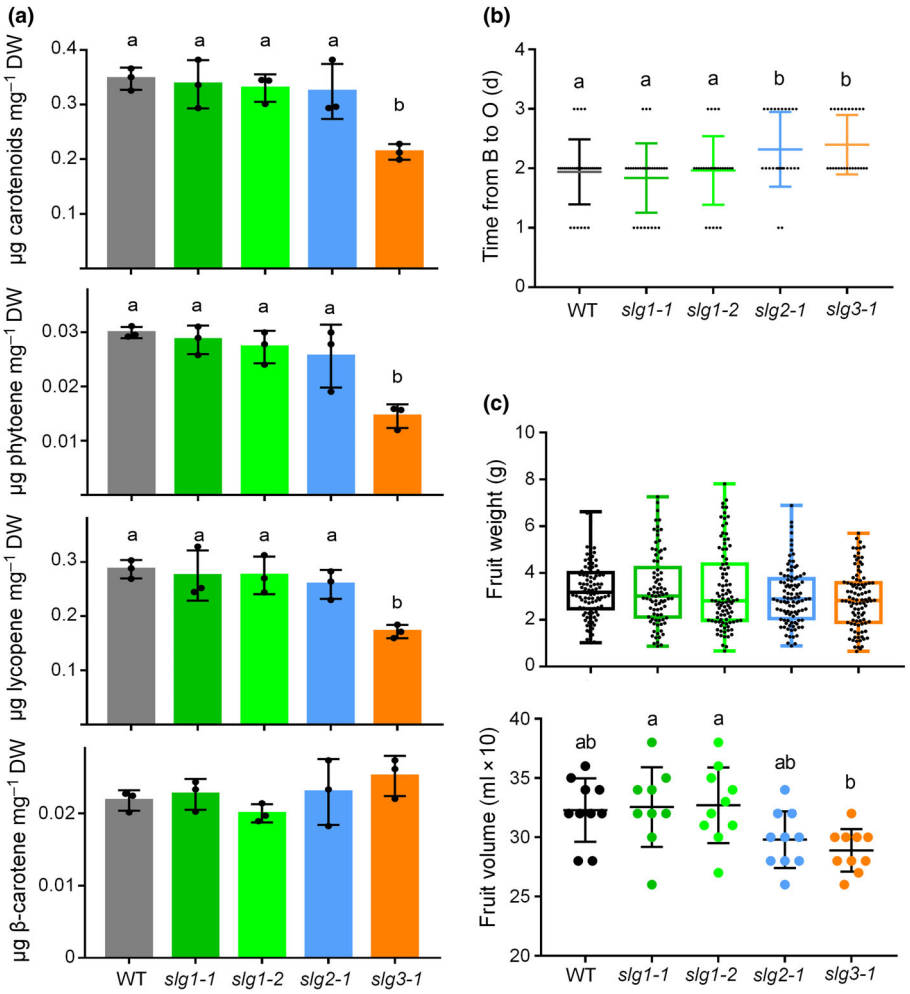

Fig. 4 SlG1 is dispensable for carotenoid biosynthesis in tomato fruits. (a) Levels of total and individual carotenoids (phytoene, lycopene, and β-carotene) in tomato fruits collected from the plant 3 d after the breaker (B) stage (B + 3). Values represent mean and SD of $n = 3$ independent biological replicates. (b) Fruit ripening rate estimated as the number of days from breaker (B) to orange (O) stages in the plant. Black dots indicate individual values, and colored lines represent the mean and the SD. (c) Weight and volume of fully ripe (R) fruits of the indicated genotypes. In the weight boxplot, the lower and upper boundary of the boxes indicate the 25th and 75th percentile, respectively; the line inside the boxes represents the median; dots mark individual data values; and whiskers above and below the boxes indicate the maximum and minimum values. In the volume dot plot, central line represents the mean and whiskers represent SD. In all cases, letters represent statistically significant differences ($P < 0.05$) among means according to *post hoc* Tukey's tests run when one-way ANOVA detected different means. WT, wild-type.

PHYTOZOME) to look for tomato homologs of genes for plastidial isoprenoid biosynthesis and related pathways. We obtained the expression data of such tomato homologs from recently published tomato RNA-Seq data in root tissue (Wang *et al.*, 2021) and calculated their expression correlation with *SlG1*, *SlG2*, and *SlG3* expression using pairwise Pearson correlations as reported previously (Wang *et al.*, 2022). Results are shown in Fig. 5, and correlations and gene details are listed in Table S3. Opposite to that observed in leaf tissue, *SlG2* displays a low correlation with other isoprenoid biosynthetic genes in roots (Fig. 5). *SlG3* shows a medium connectivity to many of the selected genes, probably because it is the isoform providing GGPP for housekeeping functions (Barja *et al.*, 2021). Intriguingly, *SlG1* expression showed a high correlation with many genes of the MEP and the carotenoid pathways as well as with most of the genes involved in SL biosynthesis, while it showed limited connectivity with genes converting carotenoids into ABA (Fig. 5). These results suggest that gene expression is coordinated such that SlG1-derived root carotenoids are channeled into the production of SLs but not ABA. *SlG1* connectivity was also very high with GA biosynthetic genes. GAs are GGPP-derived phytohormones that appear to act together with SLs during the P-starvation response (Wang *et al.*, 2021) and root mycorrhiza formation (Ruiz-Lozano *et al.*, 2016; Nouri *et al.*, 2021), promoting root growth to help establishment of AM symbiosis. A tight correlation between SLs and the expression of GA-related genes has been reported (Wang *et al.*, 2021), suggesting that the observed co-expression of *SlG1* with GA biosynthetic genes might be a secondary effect.

SlG1 specifically interacts with PSY3

Gene expression data and our GCN analysis (Fig. 5) support the conclusion that SlG1 might function in coordination with PSY3 to produce SL and likely other AM-associated apocarotenoids (but not ABA) in roots (Stauder *et al.*, 2018; Barja *et al.*, 2021). GGPPS proteins have been shown to physically interact with PSY enzymes in different plant species (Ruiz-Sola *et al.*, 2016b; Wang *et al.*, 2018; Camagna *et al.*, 2019; Barja *et al.*, 2021). In tomato, co-immunoprecipitation experiments in *N. benthamiana* leaves showed direct interaction of SlG2 with PSY1 and PSY2, while no interaction with these PSY isoforms was found for SlG3 even though the latter was shown to homodimerize and heterodimerize with SlG2 using the same experimental design (Barja *et al.*, 2021). To extend the tomato GGPPS-PSY interaction map

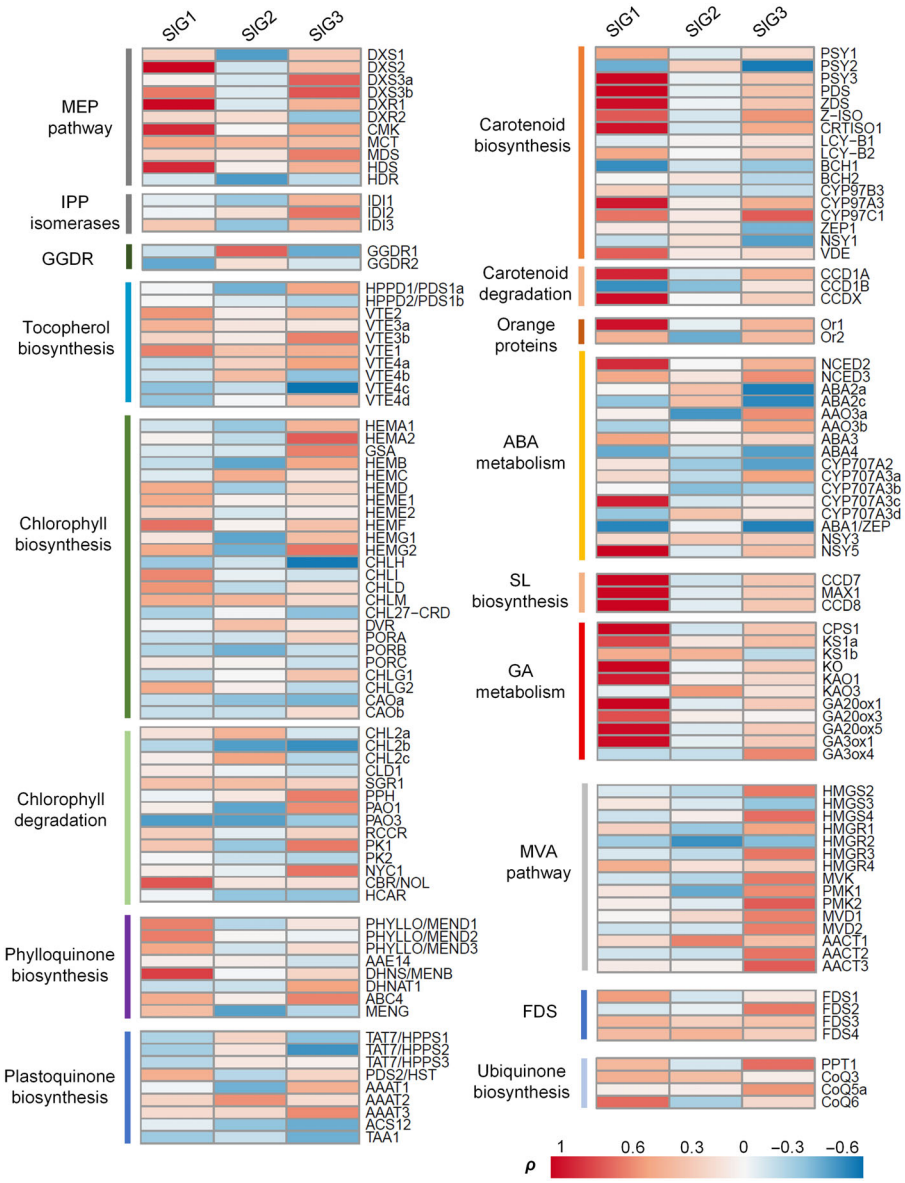

Fig. 5 *SlG1* expression is highly correlated with carotenoid and strigolactone biosynthesis in tomato roots. Heatmap represents pairwise Pearson correlations (ρ) between the expression of genes encoding geranylgeranyl diphosphate (GGPP) synthase (GGPPS) isoforms and those for the indicated enzymes from pathways upstream and downstream of GGPP. Gene details, abbreviations, accessions, and data correlations are listed in Supporting Information Table S3. ABA, abscisic acid; FDS, farnesyl diphosphate; GA, gibberellins; GGDR, geranylgeranyl diphosphate reductase; IPP, isopentenyl diphosphate; MEP, methylerythritol 4-phosphate; MVA, mevalonic acid; SL, strigolactones.

with SlG1, we performed co-immunoprecipitation assays *in planta* using Myc-tagged GGPPS and HA-tagged PSY proteins (Fig. 6). Tagged proteins were transiently expressed in *N. benthamiana* leaves by agroinfiltration, and then protein extracts were used to confirm the presence of the recombinant enzymes (Fig. 6a) and for co-immunoprecipitation with anti-Myc antibodies followed by immunoblot analysis with both anti-Myc and anti-HA antibodies (Fig. 6b). A Myc-tagged phosphoribulokinase protein from Arabidopsis (PRK-Myc) was used as a negative control (Barja *et al.*, 2021). Additionally, a SlG1-HA construct used together with SlG1-Myc confirmed that SlG1 forms homodimers and that the Myc-tagged version allowed co-immunoprecipitation of protein partners (Fig. S5). When combined with PSY isoforms, SlG1 was found to only co-immunoprecipitate with PSY3, whereas SlG2 and SlG3 were unable to interact with this particular PSY isoform (Fig. 6b).

Roots of *slg1* mutants exude less SLs under phosphate starvation

To experimentally confirm the role of SlG1 in the production of carotenoid precursors for SL biosynthesis in roots, we analyzed the levels of a number of SLs in the root exudate of WT and mutant plants. As a control, we used a tomato MicroTom line with a silenced *SlCCD7* gene (Solyc01g090660), encoding the SL biosynthetic enzyme carotenoid-cleavage dioxygenase 7 (Pino *et al.*, 2022). This line, herein named *ccd7*, shows a highly branched phenotype consistent with an expected low SL production (Pino *et al.*, 2022). We grew the plants in half-strength Hoagland solution either containing normal phosphate (+P) or without phosphate (−P) to stimulate SL biosynthesis and measured carotenoid levels in root tissues and SL levels in root exudates (Fig. 7). Carotenoid levels measured in roots were very low in all genotypes

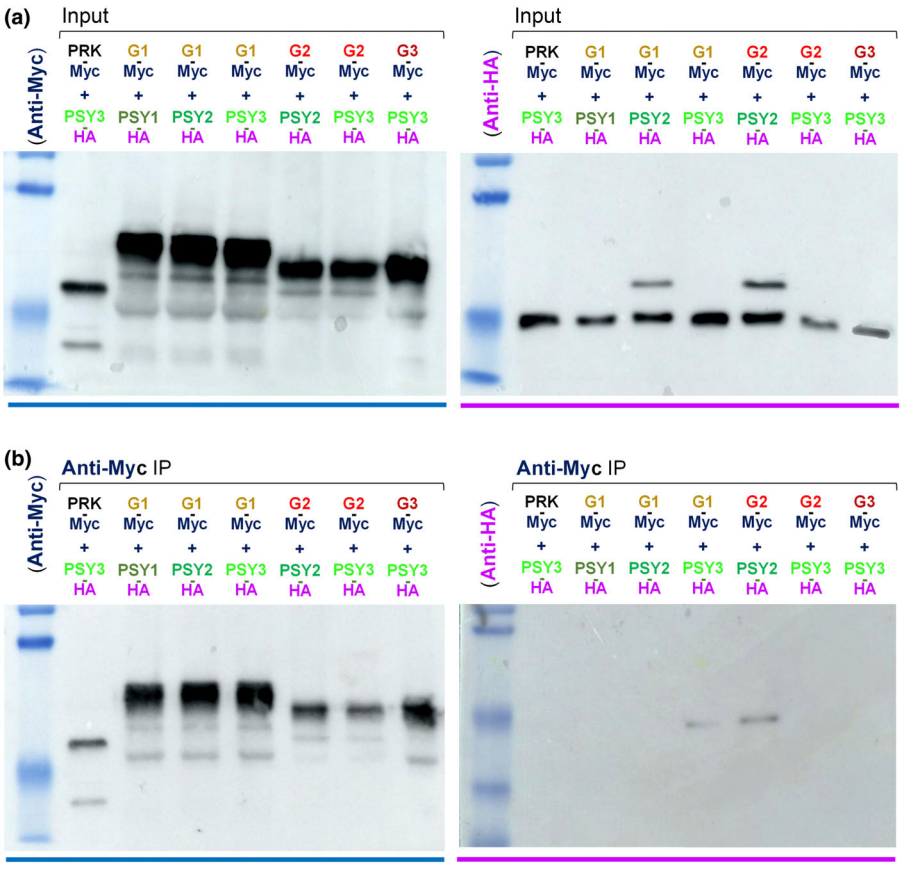

Fig. 6 SlG1 specifically interacts with PSY3 *in planta*. *Nicotiana benthamiana* leaves were co-agroinfiltrated with constructs encoding the indicated proteins tagged with C-terminal Myc or hemagglutinin (HA) epitopes. (a) Immunoblot analysis of crude extracts (INPUT) with anti-Myc (dark blue) and anti-HA (purple) antibodies to confirm successful protein production. (b) Immunoblot analysis of extracts after immunoprecipitation (IP) with anti-Myc. The same samples were used for immunodetection with anti-Myc (to confirm successful IP) or anti-HA (to identify co-immunoprecipitated partners). Predicted protein molecular weights (kDa): PRK-Myc, 52.1; SlG1-Myc, 56.9; SlG2-Myc, 55.3; SlG3-Myc, 55.5; PSY1-HA, 50.7; PSY2-HA, 51.0; PSY3-HA, 50.2.

both under +P and −P conditions (Fig. 7a). Only the *ccd7* line displayed statistically significant changes between conditions, as carotenoid levels increased under phosphate starvation (Fig. 7a). The SL levels in root exudates from plants grown under phosphate starvation for 7 d were significantly lower in both *slg1* mutant alleles compared with WT controls (Fig. 7b). The only exception was oxo-orobanchol, which showed no significant change but did display a trend toward lower levels in both SlG1-defective mutant lines. Exudates from *slg2-1* and *slg3-1* roots contained WT levels of SLs (Fig. 7b). These results confirm a major role for the SlG1 isoform in producing GGPP precursors for the carotenoid-derived SLs. Consistent with our GCN data showing no co-expression of ABA biosynthetic genes with any of the tomato genes for GGPPS isoforms (Fig. 5), none of the GGPPS-defective mutants presented statistically significant differences in root ABA levels under +P or −P conditions compared with WT controls (Fig. 7c).

PSY3-defective lines are not available yet, but we used our CRISPR-Cas9 lines lacking PSY1 (*psy1-2*) and PSY2 (*psy2-1*) (Ezquerro *et al.*, 2022) for the genetic analysis of the role of PSY isoforms in root SL biosynthesis. Because a role for PSY3 in producing carotenoid precursors for root SL production has been demonstrated in the legume *Medicago truncatula* and suggested in tomato (Stauder *et al.*, 2018), we expected WT levels of SLs in mutants defective in PSY1 and PSY2, which harbor a functional PSY3 enzyme. However, *psy1-2* displayed a very similar reduction in SL levels to that detected in *slg1*, suggesting that PSY1 may also have a role in SL biosynthesis in tomato roots (Fig. 7b). In agreement, *PSY1* basal expression levels in roots are higher than those of *PSY3* (Fantini *et al.*, 2013; Barja *et al.*, 2021). Furthermore, *PSY1* expression also increases in mycorrhized roots compared with nonmycorrhized controls (Stauder *et al.*, 2018; Barja *et al.*, 2021). Strikingly, in PSY1-defective roots *SlG1* expression was not upregulated under phosphate starvation (Fig. 8), suggesting that the low SL levels produced by the *psy1-2* mutant might be caused by the failure to induce *SlG1* expression rather than by the loss of PSY1 activity. This result further reinforces the conclusion that SlG1 has a central role in SL production in roots. Upregulation of *PSY3* expression under phosphate starvation was also reduced (but not impaired) in *psy1-2* roots, similar to that observed in SlG1-defective roots (Fig. 8). This result suggests that SLs might feedback promote *PSY3* expression. Alternatively, the absence of SlG1 (in *slg1* mutants) or the failure to upregulate its levels under phosphate starvation (in *psy1* mutants) might be the reason why *PSY3* expression also becomes less responsive to phosphate starvation. As SlG1 and PSY3 isoforms physically interact (Fig. 6), it is not surprising that their transcription is coordinated. In any case, the data strongly support a central role for SlG1 and PSY3 in root SL production.

SL reduction in *slg1* and *psy1* roots does not affect aerial plant architecture

Besides acting as soilborne signals exuded by roots, SLs of unknown identity act as plant phytohormones that regulate

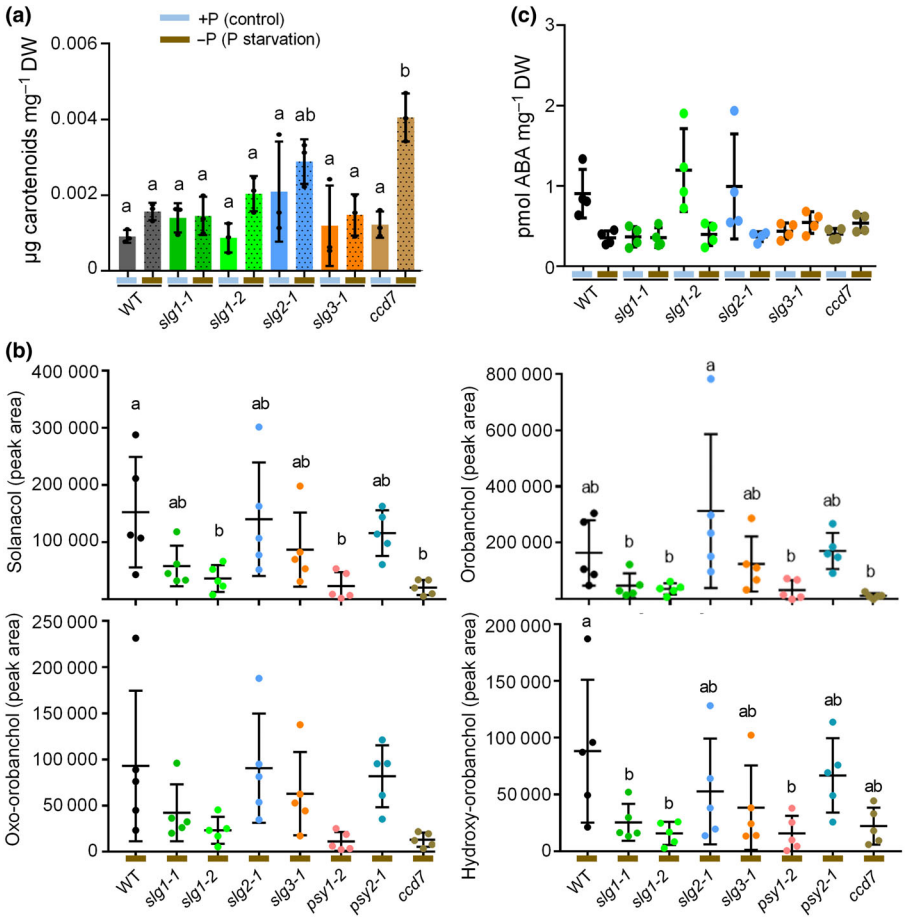

Fig. 7 SlG1 is involved in tomato root strigolactones (SL) production. Plants of the indicated genotypes were grown in half-strength Hoagland solution with normal phosphate (+P) or under phosphate starvation (−P) conditions. Samples of root tissues or exudates were collected for metabolite analyses. (a) Carotenoid levels in root tissues. Values correspond to the mean and SD of $n = 3$ independent biological replicates. (b) Levels of individual SLs in root exudates under phosphate starvation. Values represent the mean and SD of $n = 5$ independent biological replicates. In dot plots, inner line is the mean and whiskers represent SD. (c) Abscisic acid (ABA) levels in root tissues. Values correspond to mean and SD of $n = 4$ independent biological replicates. In all cases, letters represent statistically significant differences ($P < 0.05$) among means according to *post hoc* Tukey's tests run when one-way ANOVA detected different means. WT, wild-type.

endogenous developmental processes in roots, shoots, and leaves. They promote root hair elongation, lateral root outgrowth, and primary root growth and inhibit adventitious root formation (Ruyter-Spira *et al.*, 2011; Kohlen *et al.*, 2012; Al-Babili & Bouwmeester, 2015; Matthys *et al.*, 2016). In shoots, they promote secondary growth and inhibit auxiliary bud branching (Gomez-Roldan *et al.*, 2008; Ruyter-Spira *et al.*, 2013), and in leaves, they promote leaf senescence together with other plant hormones (Ueda & Kusaba, 2015; Yamada & Umehara, 2015). While increased branching is one of the most conspicuous phenotypes caused by reduced SL hormone levels, a visual inspection could not detect any obvious branching phenotype in glasshouse-grown plants of any of our CRISPR-Cas9-edited lines.

To obtain quantitative data, we measured several phenotypic parameters related to SL hormone-regulated plant growth in our edited lines grown together with WT controls and SL-deficient *ccd7* plants (Vogel *et al.*, 2010; Pino *et al.*, 2022). Measurements were performed on 15 plants per genotype grown under +P for 4 wk and then transferred to −P for two more weeks to promote SL biosynthesis (Ruyter-Spira *et al.*, 2013; Fig. 9). SL hormone biosynthesis mutants, including in tomato, are typically dwarfs with increased numbers of lateral branches (Gomez-Roldan *et al.*, 2008; Kohlen *et al.*, 2012; Yamada *et al.*, 2014; Zhang *et al.*, 2018). Consistently, we observed that *ccd7* plants were smaller than WT plants (Fig. 9a). Surprisingly, the SL-deficient mutants (*slg1-1*, *slg1-2*, and *psy1-2*) displayed a very similar size as WT plants, whereas *slg2-1* and *slg3-1*, which produced normal levels of SLs in roots, were smaller (Fig. 9a). The reduced size of *slg2-1* and *slg3-1* plants might be due to metabolic imbalances resulting from suboptimal photosynthesis (Barja *et al.*, 2021). Besides a reduced plant height, *ccd7* plants displayed a higher number of lateral branches compared with WT controls in our experimental conditions (Fig. 9b), consistent with previous reports by other groups (Vogel *et al.*, 2010; Pino *et al.*, 2022). In agreement with our preliminary visual observations, none of the mutants defective in GGPPS or PSY isoforms displayed a shoot branching phenotype (Fig. 9b). Analysis of root weight showed a reduction in SL-deficient *slg1-1*, *slg1-2*, *psy1-2*, and *cdd7* plants compared with WT controls and mutants with normal levels of SLs in the root exudate, that is, *slg2-1*, *slg3-1*, and *psy2-1* plants (Fig. 9c). These data are consistent with the proposed role of SL hormones in promoting root growth (Ruyter-Spira *et al.*, 2013; Al-Babili & Bouwmeester, 2015). To analyze *slg1* root architecture in further detail, the *slg1-1* mutant together with *ccd7* and WT controls was germinated and grown for 2 wk on vertical plates with solid medium lacking P (Fig. S6). Under these conditions, a trend toward reduced root weight was also detected in *slg1* and *ccd7* plants but it was only statistically significant in the latter. Global root length (but not area) was reduced in both SL-defective mutants, whereas primary root length was only reduced in *slg1*.

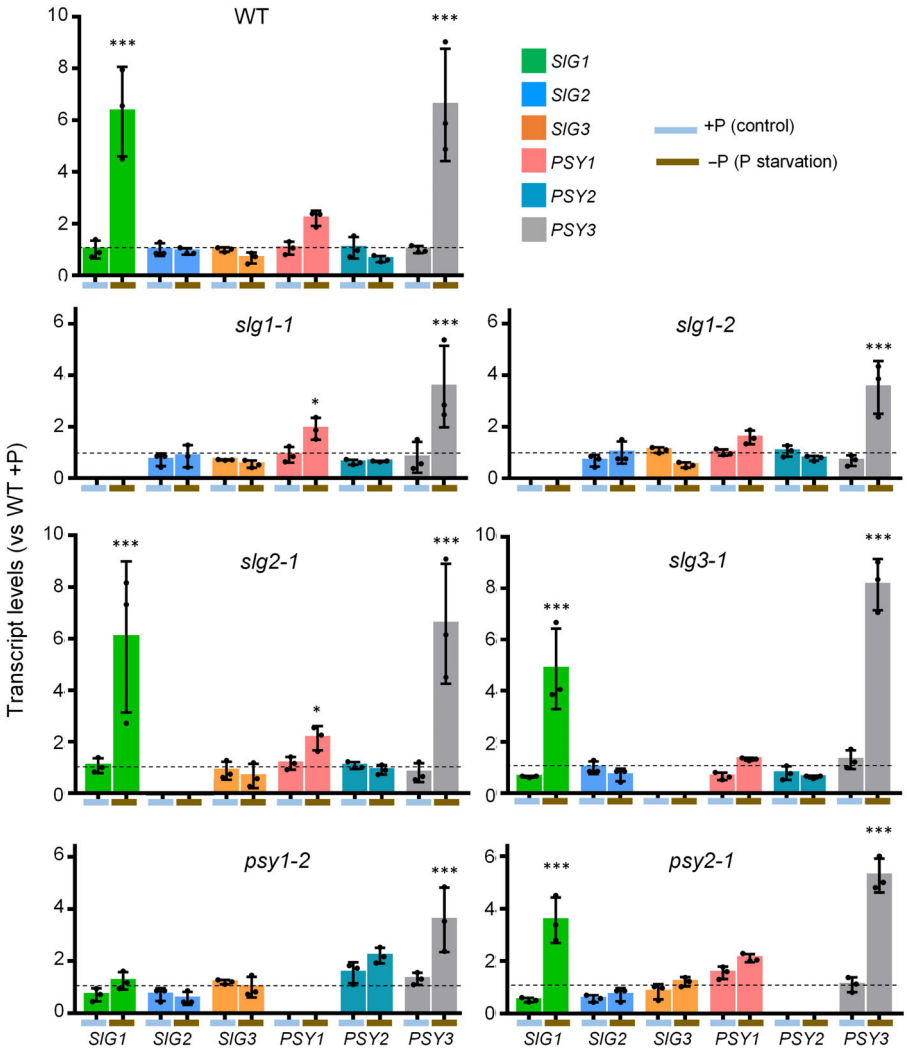

Fig. 8 Genes encoding geranylgeranyl diphosphate synthase (GGPPS) and phytoene synthase (PSY) paralogs show differential responses to phosphate starvation in tomato roots. RNA samples from roots collected from the plants described in Fig. 7 were used for RT-qPCR experiments. Transcript levels were normalized using the tomato *ACT4* gene, and they are shown relative to those in control (+P) wild-type (WT) samples (dotted line). The scale is the same in all plots to facilitate comparisons. Mean and SD of $n = 3$ independent biological replicates are shown. Asterisks indicate statistically significant differences between conditions (+P vs −P) for each gene in each genotype according to one-way ANOVA with Dunnett's multiple comparisons test: *, $P < 0.05$; ***, $P < 0.001$).

Lateral root number was significantly reduced in *ccd7* plants, consistent with the effect of SLs in Arabidopsis (Ruyter-Spira *et al.*, 2011). Together, these results show that the *slg1* mutant displays subtle developmental phenotypes in the roots but not the reduced lateral root density phenotype associated with SL hormone deficiency observed in *ccd7* plants. Both *slg1* and *ccd7* plants showed no statistically significant alterations in shoot weight (Fig. S6).

Discussion

In this work, we investigated the function of the GGPPS isoform SlG1 by generating loss-of-function lines and combining their metabolic and physiological phenotyping with gene co-expression and co-immunoprecipitation analyses. We previously showed that SlG3 plays a main role as a housekeeping isoform, whereas SlG2 acts as a helper enzyme to meet peak demands of GGPP in tomato leaves and fruit (Barja *et al.*, 2021), but the role of SlG1 remained virtually unexplored. Here, we demonstrate that SlG1 does not substantially contribute to GGPP production for carotenoid synthesis in leaf chloroplasts or fruit chromoplasts, but it plays an important role in the production of defensive diterpenes (in leaf trichomes) and SLs (in roots). While upregulation of *SlG1* expression likely helps the housekeeping isoform SlG3 to meet an increased demand of GGPP for diterpene biosynthesis in response to biotic stress, co-expression with SL biosynthetic genes in roots is expected to ensure increased SL production during phosphate starvation.

SlG1 was found to specifically interact with PSY3 (Fig. 6). It has been suggested that PSY enzymes cannot access freely diffusible plastidial GGPP because of their specific plastid location attached to membranes (Camagna *et al.*, 2019), making interaction among GGPPS and PSY enzymes necessary for GGPP channeling into the carotenoid pathway. Strikingly, the tomato housekeeping isoform SlG3 is unable to directly interact with any of the PSY isoforms present in tomato (Fig. 6b; Barja *et al.*, 2021). However, there are several possibilities for an indirect interaction of SlG3 with PSY enzymes (Barja & Rodriguez-Concepcion, 2021). Heterodimerization of SlG2 and SlG3 might allow interaction of SlG3 with PSY1 or PSY2 via SlG2 (Barja *et al.*, 2021), whereas possible heterodimerization of SlG1 and SlG3 might allow interaction with PSY3 (Fig. 6b). Another mechanism that could potentially facilitate the GGPP – PSY

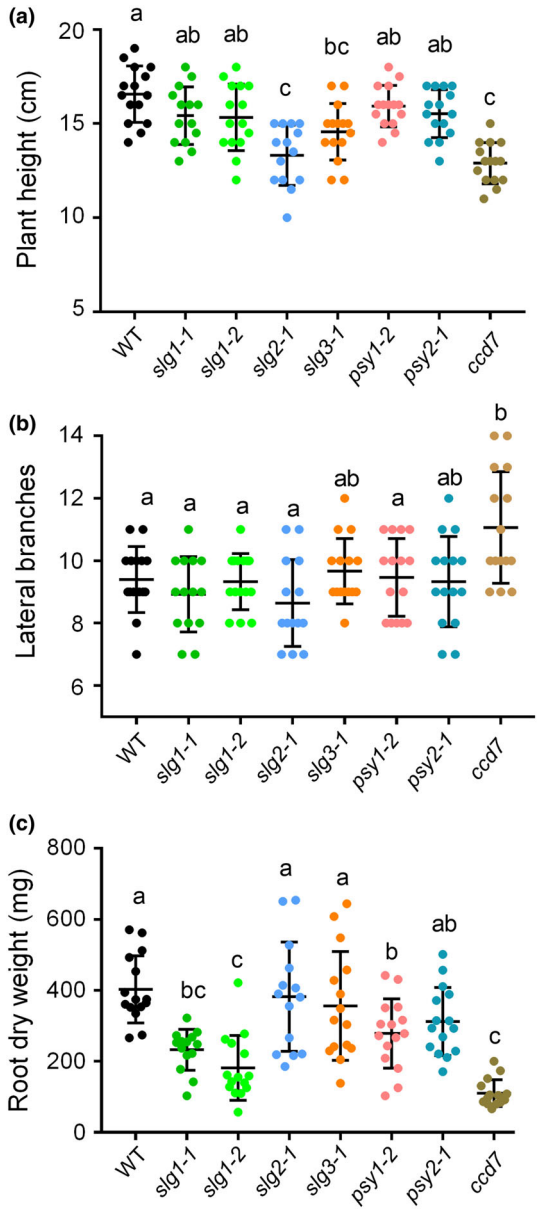

Fig. 9 Defective strigolactones (SL) synthesis in tomato *slg1* plants does not impact shoot growth or branching. Measurements were performed using plants of the indicated genotypes grown under +P for 4 wk and then transferred to −P for 2 more weeks to promote SL synthesis. (a) Plant height from the root–stem transition to the apical meristem bud. (b) Number of lateral branches arising from the main stem. (c) Weight of entire roots after freeze-drying. In all plots, dots indicate individual values, whiskers indicate mean and SD, and letters represent statistically significant differences ($P < 0.05$) among means according to *post hoc* Tukey's tests run when one-way ANOVA detected different means.

interaction could be interaction with the small subunit type II (SSU-II) protein (Solyc09g008920), a catalytically inactive polypeptide shown to interact with different GGPPS enzymes not only to improve their GGPP production (Zhou *et al.*, 2017; Wang *et al.*, 2018; Zhou & Pichersky, 2020) but also to stimulate the interaction with PSYs (Wang *et al.*, 2018). While the described interactions potentially allow any of the three tomato GGPPS isoforms to form a complex with any of the PSY isoforms, it is expected that direct interactions (SlG1-PSY3, SlG2-PSY1, and SlG2-PSY2) would be most efficient to convert GGPP into phytoene. In the case of SlG1 and PSY3, this interaction is strengthened by the coordinated expression profiles of the corresponding genes in roots upon phosphate starvation and mycorrhiza formation with AM fungi (Fig. 5; Stauder *et al.*, 2018; Barja *et al.*, 2021) and this strongly supports the conclusion that these isoforms share the same functional role(s) in providing precursors for SL biosynthesis.

The structure of the SL hormone is as yet unknown, but there is ample evidence that it differs from the structure of the SLs present in the root exudate and that it is likely derived from methylcarlactonoic acid (MeCLA; Ito *et al.*, 2022; Mashiguchi *et al.*, 2022). The biosynthesis of MeCLA in tomato has not been demonstrated yet, but there are indications that it is derived from carlactonoic acid (CLA). For example, a mutation in *SlMAX1* (not making CLA) results in a branched phenotype, while a mutation in *SlCYP722c* (still making CLA but not orobanchol) does not (Zhang *et al.*, 2018; Wakabayashi *et al.*, 2019). While disrupted SlCCD7 activity results in a branched shoot phenotype, loss of SlG1 does not, even though it does result in a much lower production of the rhizosphere signaling SLs and a root phenotype. In part, this might be explained because constitutive silencing of the *SlCCD7* gene affects the production of the SL hormone in all plant tissues, whereas loss of SlG1 appears to only affect SL production in roots. It is commonly accepted that SL hormones are synthesized in plant roots and from there transported to aerial parts, where they regulate plant growth and shoot branching (Gomez-Roldan *et al.*, 2008; Ruyter-Spira *et al.*, 2013; Al-Babili & Bouwmeester, 2015). Nevertheless, grafting studies in tomato and pea have shown that the SL biosynthetic machinery is also active in stems and can produce SLs that are then transported to shoots and leaves (Beveridge *et al.*, 2009; Xie *et al.*, 2010; Visentin *et al.*, 2016). As the expression levels of *SlG1* in aerial parts under normal conditions are very low (*c.* 40-fold lower than *SlG2* and 50-fold lower than *SlG3*; Fig. S3; Stauder *et al.*, 2018; Barja *et al.*, 2021), we propose that SlG1 is exclusively involved in providing GGPP for SL biosynthesis (both the SL hormone and the rhizosphere signaling SLs) in the roots. In shoots, much higher levels of carotenoids (derived from GGPP made by SlG2 and/or SlG3) may supply enough precursors to produce SLs supporting normal aboveground growth and development, even when SL biosynthesis in the roots is inhibited, as is the case in the *slg1* mutant.

In summary, extensive characterization of tomato lines defective in the SlG1 isoform confirmed the participation of this isoform in the production of (1) the diterpene GL and its defense-related derivative TMTT in leaves upon biotic stress (i.e. bacterial infection) and (2) SLs in roots in response to phosphate starvation. Specifically, SlG1 appears to act together with PSY3 in the roots to produce SLs but not other carotenoid-derived hormones such as ABA. SLs released by plant roots to the soil are signaling molecules for colonization by AM fungi but also a cue-inducing germination in parasitic plants (Yoneyama *et al.*, 2008; López-Ráez *et al.*, 2009; Bouwmeester *et al.*, 2021). The particular

characteristics of the *slg1* mutant make it an attractive target for breeding to negate the negative effects associated with infection by parasitic plants, but without altering normal shoot growth and metabolism, including photosynthesis and fruit ripening. The reduced emission of TMTT in the mutant, however, might have deleterious effects for plant defense.

Acknowledgements

We thank Mª Rosa Rodriguez-Goberna and the IBMCP Metabolomics Platform for technical help with HPLC analyses, Kristýna Floková for the support with ABA measurements, Ernesto Llamas for providing the pGWB417_AtPRK construct, Rodrigo Therezan and Lazaro E. P. Peres (USP, Brazil) for the tomato *ccd7* line, and Albert Ferrer and Laura Gutiérrez for the pDE-Cas9 (with kanamycin resistance) plasmid. This work was funded by grants from Spanish MCIN/AEI/10.13039/501100011033 and European NextGeneration EU/PRTR and PRIMA programs to MR-C (PID2020-115810GB-I00 and UToPIQ-PCI2021-121941). Funding was also provided by Generalitat Valenciana (PROMETEU/2021/056 and AGROALNEXT/2022/067). ME received a predoctoral fellowship from MCIN/AEI (BES-2017-080652) and an EMBO Scientific Exchange Grant (9315).

Competing interests

None declared.

Author contributions

ME and MR-C designed the research. ME, CL, JP-P, EB-E, MVB and YW performed the research. LD, MPL-G, PL and HJB contributed to the new analytic tools. ME, CL, JP-P, EB-E, MVB, YW, LD, PL, MPL-G, HJB and MR-C analyzed and discussed the data. ME and MR-C wrote the paper and incorporated the input of the rest of the authors.

ORCID

M. Victoria Barja https://orcid.org/0000-0002-3846-4885
Harro J. Bouwmeester https://orcid.org/0000-0003-0907-2732
Esteban Burbano-Erazo https://orcid.org/0000-0001-5056-9893
Lemeng Dong https://orcid.org/0000-0002-1435-1907
Miguel Ezquerro https://orcid.org/0000-0002-3051-5502
M. Pilar López-Gresa https://orcid.org/0000-0001-9251-0160
Changsheng Li https://orcid.org/0000-0002-9579-4127
Purificación Lisón https://orcid.org/0000-0002-1662-8084
Julia Pérez-Pérez https://orcid.org/0000-0001-9448-0700
Manuel Rodríguez-Concepción https://orcid.org/0000-0002-1280-2305
Yanting Wang https://orcid.org/0000-0003-1970-4158

Data availability

The data that support the findings of this study are available in the Supporting Information of this article.

References

Al-Babili S, Bouwmeester HJ. 2015. Strigolactones, a novel carotenoid-derived plant hormone. *Annual Review of Plant Biology* **66**: 161–186.

Ament K, van Schie CC, Bouwmeester HJ, Haring MA, Schuurink RC. 2006. Induction of a leaf specific geranylgeranyl pyrophosphate synthase and emission of (E,E)-4,8,12-trimethyltrideca-1,3,7,11-tetraene in tomato are dependent on both jasmonic acid and salicylic acid signaling pathways. *Planta* **224**: 1197–1208.

Barja MV, Ezquerro M, Beretta S, Diretto G, Florez-Sarasa I, Feixes E, Fiore A, Karlova R, Fernie AR, Beekwilder J *et al.* 2021. Several geranylgeranyl diphosphate synthase isoforms supply metabolic substrates for carotenoid biosynthesis in tomato. *New Phytologist* **231**: 255–272.

Barja MV, Rodriguez-Concepcion M. 2021. Plant geranylgeranyl diphosphate synthases: every (gene) family has a story. *aBIOTECH* **2**: 289–298.

Baslam M, Esteban R, García-Plazaola JI, Goicoechea N. 2013. Effectiveness of arbuscular mycorrhizal fungi (AMF) for inducing the accumulation of major carotenoids, chlorophylls and tocopherol in green and red leaf lettuces. *Applied Microbiology and Biotechnology* **97**: 3119–3128.

Beveridge CA, Dun EA, Rameau C. 2009. Pea has its tendrils in branching discoveries spanning a century from auxin to strigolactones. *Plant Physiology* **151**: 985–990.

Bouvier F, Rahier A, Camara B. 2005. Biogenesis, molecular regulation and function of plant isoprenoids. *Progress in Lipid Research* **4**: 357–429.

Bouwmeester H, Li C, Thiombiano B, Rahimi M, Dong L. 2021. Adaptation of the parasitic plant lifecycle: germination is controlled by essential host signaling molecules. *Plant Physiology* **185**: 1292–1308.

Bouwmeester HJ, Roux C, Lopez-Raez JA, Bécard G. 2007. Rhizosphere communication of plants, parasitic plants and AM fungi. *Trends in Plant Science* **12**: 224–230.

Camagna M, Grundmann A, Bar C, Koschmieder J, Beyer P, Welsch R. 2019. Enzyme fusion removes competition for geranylgeranyl diphosphate in carotenogenesis. *Plant Physiology* **179**: 1013–1027.

Chen Q, Fan D, Wang G. 2015. Heteromeric geranyl(geranyl) diphosphate synthase is involved in monoterpene biosynthesis in Arabidopsis flowers. *Molecular Plant* **8**: 1434–1437.

Degenhardt J, Köllner TG, Gershenzon J. 2009. Monoterpene and sesquiterpene synthases and the origin of terpene skeletal diversity in plants. *Phytochemistry* **70**: 1621–1637.

Ezquerro M, Burbano E, Rodríguez-Concepción M. 2022. Overlapping and specialized roles of tomato phytoene synthase isoforms PSY1 and PSY2 in carotenoid and ABA production. *bioRxiv*. doi: 10.1101/2022.08.11.503628.

Falara V, Alba JM, Kant MR, Schuurink RC, Pichersky E. 2014. Geranyllinalool synthases in solanaceae and other angiosperms constitute an ancient branch of diterpene synthases involved in the synthesis of defensive compounds. *Plant Physiology* **166**: 428–441.

Fantini E, Falcone G, Frusciante S, Giliberto L, Giuliano G. 2013. Dissection of tomato lycopene biosynthesis through virus-induced gene silencing. *Plant Physiology* **163**: 986–998.

Fester T, Schmidt D, Lohse S, Walter MH, Giuliano G, Bramley PM, Fraser PD, Hause B, Strack D. 2002. Stimulation of carotenoid metabolism in arbuscular mycorrhizal roots. *Planta* **216**: 148–154.

Gomez-Roldan V, Fermas S, Brewer PB, Puech-Pagès V, Dun EA, Pillot JP, Letisse F, Matusova R, Danoun S, Portais JC *et al.* 2008. Strigolactone inhibition of shoot branching. *Nature* **455**: 189–194.

Ito S, Braguy J, Wang JY, Yoda A, Fiorilli V, Takahashi I, Jamil M, Felemban A, Miyazaki S, Mazzarella T *et al.* 2022. Canonical strigolactones are not the major determinant of tillering but important rhizospheric signals in rice. *Science Advances* **8**: eadd1278.

Kohlen W, López Ráez JA, Pollina T, Lammers M, Toth P, Charnikhova T, de Maagd R, Pozo MJ, Bouwmeester H, Ruyter-Spira C. 2012. The tomato

CAROTENOID CLEAVAGE DIOXYGENASE8 (SlCCD8) is regulating rhizosphere signaling, plant architecture and reproductive development through strigolactone biosynthesis. *New Phytologist* **196**: 535–547.

Liu H, Ding Y, Zhou Y, Jin W, Xie K, Chen LL. 2017. CRISPR-P 2.0: an improved CRISPR-Cas9 tool for genome editing in plants. *Molecular Plant* **10**: 530–532.

López-Gresa MP, Payá C, Ozáez M, Rodrigo I, Conejero V, Klee H, Bellés JM, Lisón P. 2018. A new role for green leaf volatile esters in tomato stomatal defense against *Pseudomonas syringe* pv. tomato. *Frontiers in Plant Science* **9**: 1855–1869.

López-Ráez JA, Matusova R, Cardoso C, Jamil M, Charnikhova T, Kohlen W, Carolien RS, Verstappen F, Bouwmeester H. 2009. Strigolactones: ecological significance and use as a target for parasitic plant control. *Pest Management Science* **65**: 471–477.

Mashiguchi K, Seto Y, Onozuka Y, Suzuki S, Takemoto K, Wang Y, Dong L, Asami K, Noda R, Kisugi T *et al.* 2022. A carlactonoic acid methyltransferase that contributes to the inhibition of shoot branching in Arabidopsis. *Proceedings of the National Academy of Sciences, USA* **119**: e2111565119.

Matthys C, Walton A, Struk S, Stes E, Boyer FD, Gevaert K, Goormachtig S. 2016. The whats, the wheres and the hows of strigolactone action in the roots. *Planta* **243**: 1327–1337.

McQuinn RP, Gapper NE, Gray AG, Zhong S, Tohge T, Fei Z, Fernie AR, Giovannoni JJ. 2020. Manipulation of ZDS in tomato exposes carotenoid- and ABA-specific effects on fruit development and ripening. *Plant Biotechnology Journal* **18**: 2210–2224.

Moreno JC, Mi J, Alagoz Y, Al-Babili S. 2021. Plant apocarotenoids: from retrograde signaling to interspecific communication. *The Plant Journal* **105**: 351–375.

Nouri E, Surve R, Bapaume L, Stumpe M, Chen M, Zhang Y, Ruyter-Spira C, Bouwmeester H, Glauser G, Bruisson S *et al.* 2021. Phosphate suppression of arbuscular mycorrhizal symbiosis involves gibberellic acid signaling. *Plant and Cell Physiology* **62**: 959–970.

Pino LE, Lima JE, Vicente MH, de Sá AFL, Pérez-Alfocea F, Albacete A, Costa JL, Werner T, Schmülling T, Freschi L *et al.* 2022. Increased branching independent of strigolactone in cytokinin oxidase 2-overexpressing tomato is mediated by reduced auxin transport. *Molecular Horticulture* **2**: 12.

Pulido P, Perello C, Rodriguez-Concepcion M. 2012. New insights into plant isoprenoid metabolism. *Molecular Plant* **5**: 964–967.

Rodriguez-Concepcion M, Avalos J, Bonet ML, Boronat A, Gomez-Gomez L, Hornero-Mendez D, Limon MC, Meléndez-Martínez AJ, Olmedilla-Alonso B, Palou A *et al.* 2018. A global perspective on carotenoids: metabolism, biotechnology, and benefits for nutrition and health. *Progress in Lipid Research* **70**: 62–93.

Ruiz-Lozano JM, Aroca R, Zamarreño ÁM, Molina S, Andreo-Jiménez B, Porcel R, García-Mina JM, Ruyter-Spira C, López-Ráez JA. 2016. Arbuscular mycorrhizal symbiosis induces strigolactone biosynthesis under drought and improves drought tolerance in lettuce and tomato. *Plant, Cell & Environment* **39**: 441–452.

Ruiz-Sola MÁ, Barja MV, Manzano D, Llorente B, Schipper B, Beekwilder J, Rodriguez-Concepcion M. 2016a. A single Arabidopsis gene encodes two differentially targeted geranylgeranyl diphosphate synthase isoforms. *Plant Physiology* **172**: 1393–1402.

Ruiz-Sola MÁ, Coman D, Beck G, Barja MV, Colinas M, Graf A, Welsch R, Rütimann P, Bühlmann P, Bigler L *et al.* 2016b. Arabidopsis GERANYLGERANYL DIPHOSPHATE SYNTHASE 11 is a hub isozyme required for the production of most photosynthesis-related isoprenoids. *New Phytologist* **209**: 252–264.

Ruiz-Sola MÁ, Rodríguez-Concepción M. 2012. Carotenoid biosynthesis in Arabidopsis: a colorful pathway. *The Arabidopsis Book* **10**: e0158.

Ruyter-Spira C, Al-Babili S, van der Krol S, Bouwmeester H. 2013. The biology of strigolactones. *Trends in Plant Science* **18**: 72–83.

Ruyter-Spira C, Kohlen W, Charnikhova T, van Zeijl A, van Bezouwen L, de Ruijter N, Cardoso C, Lopez-Raez JA, Matusova R, Bours R *et al.* 2011. Physiological effects of the synthetic strigolactone analog GR24 on root system architecture in Arabidopsis: another below-ground role for strigolactones? *Plant Physiology* **155**: 721–734.

Schuurink R, Tissier A. 2020. Glandular trichomes: micro-organs with model status*? New Phytologist* **225**: 2251–2266.

Stauder R, Welsch R, Camagna M, Kohlen W, Balcke GU, Tissier A, Walter MH. 2018. Strigolactone levels in dicot roots are determined by an ancestral symbiosis-regulated clade of the PHYTOENE SYNTHASE gene family. *Frontiers in Plant Science* **9**: 255–271.

Tholl D. 2015. Biosynthesis and biological functions of terpenoids in plants. *Advances in Biochemical Engineering/Biotechnology* **148**: 63–106.

Thulasiram HV, Poulter CD. 2006. Farnesyl diphosphate synthase: the art of compromise between substrate selectivity and stereoselectivity. *Journal of the American Chemical Society* **128**: 15819–15823.

Ueda H, Kusaba M. 2015. Strigolactone regulates leaf senescence in concert with ethylene in Arabidopsis. *Plant Physiology* **169**: 138–147.

Visentin I, Vitali M, Ferrero M, Zhang Y, Ruyter-Spira C, Novák O, Strnad M, Lovisolo C, Schubert A, Cardinale F. 2016. Low levels of strigolactones in roots as a component of the systemic signal of drought stress in tomato. *New Phytologist* **212**: 954–963.

Vogel JT, Walter MH, Giavalisco P, Lytovchenko A, Kohlen W, Charnikhova T, Simkin AJ, Goulet C, Strack D, Bouwmeester HJ *et al.* 2010. SlCCD7 controls strigolactone biosynthesis, shoot branching and mycorrhiza-induced apocarotenoid formation in tomato. *The Plant Journal* **61**: 300–311.

Wakabayashi T, Hamana M, Mori A, Akiyama R, Ueno K, Osakabe K, Osakabe Y, Suzuki H, Takikawa H, Mizutani M *et al.* 2019. Direct conversion of carlactonoic acid to orobanchol by cytochrome P450 CYP722C in strigolactone biosynthesis. *Science Advances* **5**: eaax9067.

Wang Q, Huang XQ, Cao TJ, Zhuang Z, Wang R, Lu S. 2018. Heteromeric geranylgeranyl diphosphate synthase contributes to carotenoid biosynthesis in ripening fruits of red pepper (*Capsicum annuum* var. *conoides*). *Journal of Agricultural and Food Chemistry* **66**: 11691–11700.

Wang Y, Durairaj J, Duran HGS, van Velzen R, Flokova K, Liao CY, Chojnacka A, MacFarlane S, Schranz ME, Medema MH *et al.* 2022. The tomato cytochrome P450 CYP712G1 catalyses the double oxidation of orobanchol en route to the rhizosphere signalling strigolactone, solanacol. *New Phytologist* **235**: 1884–1899.

Wang Y, Duran HGS, van Haarst JC, Schijlen EG, Ruyter-Spira C, Medema MH, Dong L, Bouwmeester HJ. 2021. The role of strigolactones in P deficiency induced transcriptional changes in tomato roots. *BMC Plant Biology* **21**: 1–21.

Xie X, Yoneyama K, Yoneyama K. 2010. The strigolactone story. *Annual Review of Phytopathology* **48**: 93–117.

Yamada Y, Furusawa S, Nagasaka S, Shimomura K, Yamaguchi S, Umehara M. 2014. Strigolactone signaling regulates rice leaf senescence in response to a phosphate deficiency. *Planta* **240**: 399–408.

Yamada Y, Umehara M. 2015. Possible roles of strigolactones during leaf senescence. *Plants* **4**: 664–677.

Yoneyama K, Xie X, Sekimoto H, Takeuchi Y, Ogasawara S, Akiyama K, Hayashi H, Yoneyama K. 2008. Strigolactones, host recognition signals for root parasitic plants and arbuscular mycorrhizal fungi, from Fabaceae plants. *New Phytologist* **179**: 484–494.

Zhang M, Yuan B, Leng P. 2009. The role of ABA in triggering ethylene biosynthesis and ripening of tomato fruit. *Journal of Experimental Botany* **60**: 1579–1588.

Zhang Y, Cheng X, Wang Y, Díez-Simón C, Flokova K, Bimbo A, Bouwmeester HJ, Ruyter-Spira C. 2018. The tomato MAX1 homolog, SlMAX1, is involved in the biosynthesis of tomato strigolactones from carlactone. *New Phytologist* **219**: 297–309.

Zhang Y, van Dijk ADJ, Scaffidi A, Flematti GR, Hofmann M, Charnikhova T, Verstappen F, Hepworth J, van der Krol S, Leyser O *et al.* 2014. Rice cytochrome P450 MAX1 homologs catalyze distinct steps in strigolactone biosynthesis. *Nature Chemical Biology* **10**: 1028–1033.

Zhou F, Pichersky E. 2020. The complete functional characterisation of the terpene synthase family in tomato. *New Phytologist* **226**: 1341–1360.

Zhou F, Wang CY, Gutensohn M, Jiang L, Zhang P, Zhang D, Dudareva N, Lu S. 2017. A recruiting protein of geranylgeranyl diphosphate synthase controls metabolic flux toward chlorophyll biosynthesis in rice. *Proceedings of the National Academy of Sciences, USA* **114**: 6866–6871.

Supporting Information

Additional Supporting Information may be found online in the Supporting Information section at the end of the article.

Fig. S1 DNA sequence alignment of *SlG1* CRISPR mutants.

Fig. S2 Protein alignments of SlG1 wild-type sequences with the selected CRISPR 20 mutants.

Fig. S3 *SlG1*, *SlG2*, and *SlG3* transcript levels in different tissues and developmental stages.

Fig. S4 Expression levels of genes encoding GLS and GGPPS isoforms in leaves after *Pseudomonas syringae* infection.

Fig. S5 SlG1-Myc is able to specifically bind to protein partners.

Fig. S6 Root parameters in SL-defective mutants.

Methods S1 Metabolite analyses.

Methods S2 Gene expression analyses.

Methods S3 Co-immunoprecipitation assays.

Table S1 List of primers used in this work.

Table S2 Constructs and cloning details.

Table S3 Co-expression of tomato GGPPS paralogs (guide genes) with isoprenoid-related genes (query genes) in root tissue.

Please note: Wiley is not responsible for the content or functionality of any Supporting Information supplied by the authors. Any queries (other than missing material) should be directed to the *New Phytologist* Central Office.